

Database of Geneva stellar evolution tracks and isochrones for $(UBV)_J(RI)_C$ JHKLL'M, HST-WFPC2, Geneva and Washington photometric systems*

T. Lejeune^{1,2} and D. Schaerer³

¹ Observatório Astronómico da Universidade de Coimbra, Santa Clara, 3040 Coimbra, Portugal

² Astronomisches Institut der Universität Basel, Venusstr. 7, 4102 Binningen, Switzerland

³ Observatoire Midi-Pyrénées, Laboratoire d'Astrophysique, UMR 5572, 14 avenue E. Belin, 31400 Toulouse, France

Received 28 July 2000 / Accepted 3 November 2000

Abstract. We have used an updated version of the empirically and semi-empirically calibrated *BaSeL* library of synthetic stellar spectra of Lejeune et al. (1997, 1998) and Westera et al. (1999) to calculate synthetic photometry in the $(UBV)_J(RI)_C$ JHKLL'M, HST-WFPC2, Geneva, and Washington systems for the entire set of non-rotating Geneva stellar evolution models covering masses from 0.4–0.8 to 120–150 M_\odot and metallicities $Z = 0.0004$ ($1/50 Z_\odot$) to 0.1 ($5 Z_\odot$). The results are provided in a database which includes all individual stellar tracks and the corresponding isochrones covering ages from 10^3 yr to 16–20 Gyr in time steps of $\Delta \log t = 0.05$ dex. The database also includes a new grid of stellar tracks of very metal-poor stars ($Z = 0.0004$) from 0.8–150 M_\odot calculated with the Geneva stellar evolution code.

Key words. stars: general – stars: evolution – stars: Hertzsprung-Russell diagram – stars: fundamental parameters

1. Introduction

Studies of individual stars and resolved stellar populations are fundamental for a wide variety of astrophysical subjects. In most cases photometric observations, obtained in various systems, represent the main observable. To translate these observables into fundamental stellar parameters (mainly effective temperature, luminosity) one first has to rely on stellar atmosphere models. In a second step the observations can then be compared to stellar evolution models and interpreted in physical terms such as mass, age, composition etc. Only in rare cases (very low mass stars, Baraffe et al. 1995; O stars, Schaerer et al. 1996) stellar evolution and atmosphere models are coupled and predict thus directly observables such as colors, magnitudes etc.

Extensive grids of stellar tracks covering the most important evolutionary phases and a large metallicity range have become available in the nineties (see e.g. compilation in Leitherer et al. 1996). In addition, recent efforts have been undertaken to provide accurate synthetic colours

from grids of atmosphere models covering the bulk of the parameter space occupied by observed stars of spectral types from O to M and all luminosity classes (Lejeune et al. 1997, 1998; Bessell et al. 1998). With the availability of such data it now becomes feasible to systematically convert stellar tracks of all stellar masses and derived isochrones to a variety of photometric systems. To provide such a tool is the main goal of our database.

Existing grids, partly fulfilling this aim, include the library of Padova isochrones with *UBVRIJHK* photometry for ages ~ 4 Myr–20 Gyr and metallicities Z between 0.0004 and 0.05 (Bertelli et al. 1994; Girardi et al. 1996), the recent α -element enhanced tracks and isochrones of Salasnich et al. (2000) with *UBVRIJHK* and HST-WFPC2 photometry, and various other calculations covering smaller fractions of the parameter space.

For the present work we rely on an updated version of the hybrid library of synthetic stellar spectra compiled by Lejeune et al. (1997, 1998), which is corrected to match empirical colour–temperature relations at solar metallicity and semi-empirically corrected at other metallicities. These atmosphere models are used to derive synthetic photometry of the $(UBV)_J(RI)_C$ JHKLL'M, WFPC2, Geneva, and Washington systems, using proper reference spectra for the zero points and up-to-date filter

Send offprint requests to: D. Schaerer,
e-mail: schaerer@ast.obs-mip.fr

* The data base is available at CDS via anonymous ftp to [cdsarc.u-strasbg.fr](ftp://cdsarc.u-strasbg.fr) (130.79.128.5) or via <http://cdsweb.u-strasbg.fr/cgi-bin/qcat?J/A+A/366/538>

curves. This procedure is applied to essentially the full set of Geneva stellar evolution models to yield the photometric data for these systems for 1) individual stellar tracks in the mass range from 0.4–0.8 to 120–150 M_{\odot} and metallicities $Z = 0.0004$ ($1/50 Z_{\odot}$) to 0.1 ($5 Z_{\odot}$), and 2) corresponding isochrones covering ages from ~ 0 to 16–20 Gyr.

The input tracks, atmosphere models, and the synthetic photometry are described in Sect. 2. The resulting database products (tracks and isochrones) are presented in Sect. 3. Concluding remarks on the use of the various database sets are given in Sect. 4. The Appendix includes the relevant data for a previously unpublished set of stellar tracks at $Z = 0.0004$.

2. Input

2.1. Stellar models

The current compilation includes all grids of Geneva stellar evolution models published between 1992 and march 1999 in Papers I–VIII (see footnote of Table 1 for complete references) and a new grid of stellar models for very low metallicity ($Z = 1/50 Z_{\odot}$, see Appendix). Pre-main sequence models are not included (but cf. Bernasconi 1996 and Paper VIII). The complete set including the references, a grid number used subsequently throughout the paper, and other main characteristics are listed in Table 1 (see the original papers for a full description).

The physical ingredients have been discussed in Papers I–VIII. For completeness sake a brief summary of the basic assumptions common to most model sets is presented here. Variations are discussed below. 1) OPAL and low temperature opacities of Kurucz (1991) or Alexander & Ferguson (1994) are used. 2) The initial (Y, Z) composition is derived from a linear chemical enrichment law $Y = Y_{\text{P}} + (\Delta Y/\Delta Z)Z$ with $Y_{\text{P}} = 0.24$, and $\Delta Y/\Delta Z = 3$ for $Z \leq 0.02$ and $\Delta Y/\Delta Z = 2.5$ for $Z > 0.02$ respectively. 3) Mass loss rates are taken from de Jager et al. (1998) throughout the HR-diagram except on the red giant branch (RGB) and early asymptotic giant branch (EAGB) for initial masses $M < 5 M_{\odot}$, where the following expression is used (cf. Reimers 1975): $\dot{M} = 4 \cdot 10^{-13} \eta LR/M$ in units of $M_{\odot} \text{ yr}^{-1}$, with $\eta = 0.5$ at solar metallicity (see Maeder & Meynet 1989). Mass loss is scaled with metallicity by $(Z/Z_{\odot})^{0.5}$, except for Wolf-Rayet (WR) stars. In the WR phases the relation of Langer (1989) for WNE and WC stars, and $\dot{M} = 4 \cdot 10^{-5} M_{\odot} \text{ yr}^{-1}$ for WNL stars is used. 4) Moderate core overshooting of $d_{\text{over}}/H_{\text{P}} = 0.2$ is included for stars $M \geq 1.5 M_{\odot}$. For stars at $M = 1.25 M_{\odot}$ with a small or absent convective core tracks with and without overshooting are provided. 5) In addition to the effects treated by Maeder & Meynet (1989), partial ionisation of heavy elements is included in the equation of state. 6) Optically thick envelopes of WR stars are treated in the framework of the modified Castor et al. (CAK, 1975) theory.

The above ingredients are used in grids 2–7 which cover the metallicity range from $Z = 0.001$ to 0.100 ($1/20$ – $5 Z_{\odot}$). Grids 1 and 8–12 were calculated with mass loss rates enhanced by a factor of 2 during the MS, the pre-WR, and WNL phases for massive stars (range indicated in Col. 6); for lower masses the models are complemented with the tracks from grids 2–6 or represent new calculations (grid 1; see Appendix). In grids 1–12, depending on the stellar mass range, the evolution is in general followed up to the following phases: to the end of C-burning for massive stars ($M \geq 7 M_{\odot}$), to the end of the early asymptotic giant branch (EAGB) for intermediate mass stars ($2 \leq M/M_{\odot} \leq 5$), and up to before the helium flash for low mass stars ($0.8 \leq M/M_{\odot} \leq 1.7$). Grids 13 and 14 (Paper VI) present new calculations for the latter mass range at metallicities $Z = 0.020$ and 0.001 including post-helium flash models, i.e. covering the horizontal branch (HB) and EAGB phases. The post-helium flash tracks do not include overshooting and semi-convection. The MHD (Mihalas et al. 1988) equation of state was used for the low mass models of Paper VIII (grids 15–17). The calculations in grids 15–17 are followed up to before the helium flash or ages larger than the Hubble time ($\gtrsim 20$ Gyr). Note that the solar metallicity grid 16 uses a different Y/Z composition than the remaining $Z = 0.020$ grids.

The present compilation includes stellar models covering a very large parameter space in terms of mass, metallicity, and evolutionary phases. However, we wish to stress again that e.g. the following evolutionary phases are not covered: 1) pre-main sequence tracks (for Geneva models see Bernasconi 1996 and Paper VIII), 2) thermally pulsing AGB stars, and 3) post-AGB stars and white dwarfs. Other phases (e.g. horizontal branch) are given only for a subset of metallicities. These limitations should be recognized by the user of the database. Calculations from other groups partly including such phases are mentioned in Sect. 4.

2.2. Atmosphere models

The conversion of the theoretical tracks and isochrones of the present compilation to observational colour-magnitude (c-m) diagrams has been performed using the stellar spectral library of Lejeune et al. (1997, 1998) that provides empirically and semi-empirically *colour-calibrated* model atmosphere spectra for a large range of fundamental stellar parameters, T_{eff} (2000 K to 50 000 K), $\log g$ (–1.0 to 5.5), and $[\text{Fe}/\text{H}]$ (5.0 to +1.0).

For the present calculations, we use the most recent version of this library (Westera et al. 1999), *BaSeL-2.2*¹, in which (1) all the model spectra of stars with $T_{\text{eff}} \geq 10\,000$ K are now calibrated upon empirical colours from

¹ The *BaSeL-1.0* and *BaSeL-2.0* libraries were published in Lejeune et al. (1997) and Lejeune et al. (1998) respectively, while *BaSeL-2.2* is available only electronically at <ftp://ftp.astro.unibas.ch/pub/lejeune/>. See also this ftp site for a description of the changes in the different versions.

Table 1. Summary of stellar grids included in the database. The grid number used throughout the paper (Col. 1), database ID (2), initial chemical composition (3–5), indications on the mass loss prescription (6), the covered mass range (7), the reference for the tracks (8), and a brief description of the main characteristics (9) are given

Grid #	database ID	Z	X	Y	\dot{M}	mass range	paper ^(*)	description
(1)	(2)	(3)	(4)	(5)	(6)	(7)	(8)	(9)
Basic grids:								
1	e	0.0004	0.7584	0.2412	$2 \times \text{std}$	0.8–150 M_{\odot}	this paper	basic grid
2	c	0.001	0.756	0.243	standard	0.8–120 M_{\odot}	I	basic grid
3	c	0.004	0.744	0.252	standard	0.8–120 M_{\odot}	III	basic grid
4	c	0.008	0.728	0.264	standard	0.8–120 M_{\odot}	II	basic grid
5	c	0.020	0.680	0.300	standard	0.8–120 M_{\odot}	I	basic grid
6	c	0.040	0.620	0.340	standard	0.8–120 M_{\odot}	IV	basic grid
7	c	0.100	0.420	0.480	standard	0.8–60 M_{\odot}	VII	basic grid
Extended grids:								
8	e	0.001	0.756	0.243	$2 \times \text{std}$: $M \geq 25 M_{\odot}$	0.8–120 M_{\odot}	V, I	high mass loss for massive stars
9	e	0.004	0.744	0.252	$2 \times \text{std}$: $M \geq 20 M_{\odot}$	0.8–120 M_{\odot}	V, III	high mass loss for massive stars
10	e	0.008	0.728	0.264	$2 \times \text{std}$: $M \geq 15 M_{\odot}$	0.8–120 M_{\odot}	V, II	high mass loss for massive stars
11	e	0.020	0.680	0.300	$2 \times \text{std}$: $M \geq 15 M_{\odot}$	0.8–120 M_{\odot}	V, I	high mass loss for massive stars
12	e	0.040	0.620	0.340	$2 \times \text{std}$: $M \geq 12 M_{\odot}$	0.8–120 M_{\odot}	V, IV	high mass loss for massive stars
13	p	0.001	0.756	0.243	standard	0.8–1.7 M_{\odot}	VI	including HB and EAGB
14	p	0.020	0.680	0.300	standard	0.8–1.7 M_{\odot}	VI	including HB and EAGB
15	m	0.001	0.756	0.243	standard	0.4–1.0 M_{\odot}	VIII	MHD equation of state
16	m	0.020	0.700	0.280	standard	0.4–1.0 M_{\odot}	VIII	MHD equation of state
17		0.020	0.680	0.300	standard	0.4–1.0 M_{\odot}	VIII	MHD equation of state
Alternate and combined model sets:								
	o	0.0004	0.7584	0.2412	$2 \times \text{std}$	0.8–2.5 M_{\odot}	this paper	no overshooting: 1.25 M_{\odot}
	o	0.001	0.756	0.243	standard	0.8–2.5 M_{\odot}	I	no overshooting: 1.25 M_{\odot}
	o	0.004	0.744	0.252	standard	0.8–2.5 M_{\odot}	III	no overshooting: 1.25 M_{\odot}
	o	0.008	0.728	0.264	standard	0.8–2.5 M_{\odot}	II	no overshooting: 1.25 M_{\odot}
	o	0.020	0.680	0.300	standard	0.8–2.5 M_{\odot}	I	no overshooting: 1.25 M_{\odot}
	o	0.040	0.620	0.340	standard	0.8–2.5 M_{\odot}	IV	no overshooting: 1.25 M_{\odot}
	l	0.001	0.756	0.243	standard	0.4–2.5 M_{\odot}		combination: grids 15, 13, 2
	l	0.020	0.680	0.300	standard	0.4–2.5 M_{\odot}		combination: grids 17, 14, 5

(*) I: Schaller et al. (1992), V: Meynet et al. (1994),
 II: Schaerer et al. (1993), VI: Charbonnel et al. (1996),
 III: Charbonnel et al. (1993), VII: Mowlavi et al. (1998a),
 IV: Schaerer et al. (1993), VIII: Charbonnel et al. (1999).

the T_{eff} versus $(B - V)$ relation of Flower (1996), and (2) the calibration procedure for the cool giant model spectra has been extended to the parameter ranges $2500 \text{ K} \leq T_{\text{eff}} < 6000 \text{ K}$ and $-1.0 \leq \log g < 3.5^2$, with in particular the effect to provide redder model colours for giants, in better

agreement with observed red giant branches of metal-poor globular clusters (see Lejeune & Buser 1999).

2.3. Synthetic photometry

In order to transform the theoretical quantities (L, T_{eff}) into magnitudes and colours, we first compute, by

² In the previous versions of the *BaSeL* models, we adopted $T_{\text{eff}} = 5000 \text{ K}$ and $\log g = 2.5$ as the upper limits for the calibration of giants (see Lejeune et al. 1998 for details).

Table 2. Summary of isochrone sets included in the database. The database ID (Col. 1), metallicity (2), and a brief description of the main characteristics (5) are indicated. The logarithmic age range (in years) covered by the isochrones is given in Cols. 3 and 4. Isochrones are provided for time steps of $\Delta \log t = 0.05$ for ages above 1 Myr ($\log t = 6.0$). For younger ages isochrones are for $\log t = 3.0, 5.0, 5.3, 5.6, 5.8,$ and 5.9 yr

Database ID	Z	age range ($\log t$)		description
(1)	(2)	from (3)	to (4)	(5)
Basic grids:				
e	0.0004	3.00	10.20	basic grid
c	0.001	3.00	10.20	basic grid
c	0.004	3.00	10.20	basic grid
c	0.008	3.00	10.20	basic grid
c	0.020	3.00	10.20	basic grid
c	0.040	3.00	10.20	basic grid
c	0.100	3.00	10.20	basic grid
Extended grids:				
e	0.001	3.00	7.50	high mass loss for massive stars
e	0.004	3.00	7.50	high mass loss for massive stars
e	0.008	3.00	7.50	high mass loss for massive stars
e	0.020	3.00	7.50	high mass loss for massive stars
e	0.040	3.00	7.50	high mass loss for massive stars
p	0.001	9.00	10.20	including HB and EAGB phases for low mass stars
p	0.020	9.00	10.20	including HB and EAGB phases for low mass stars
m	0.001	9.00	10.30	MHD equation of state for low mass stars
m	0.020	9.00	10.30	MHD equation of state for low mass stars
Alternate and combined model sets:				
o	0.0004	9.00	10.20	no overshooting: $1.25 M_{\odot}$
o	0.001	9.00	10.20	no overshooting: $1.25 M_{\odot}$
o	0.004	9.00	10.20	no overshooting: $1.25 M_{\odot}$
o	0.008	9.00	10.20	no overshooting: $1.25 M_{\odot}$
o	0.020	9.00	10.20	no overshooting: $1.25 M_{\odot}$
o	0.040	9.00	10.20	no overshooting: $1.25 M_{\odot}$
l	0.001	9.00	10.30	combination “best” low mass star models
l	0.020	9.00	10.30	combination “best” low mass star models

interpolation in the *BaSeL* grid (T_{eff} , $\log g$, and $[\text{Fe}/\text{H}]$)³ the model spectrum at each point along the track or the isochrone, and then derive the synthetic photometry by convolving the resulting flux distribution with the filter transmission functions (as given in the following sections).

The Wolf-Rayet phases in the stellar tracks are excluded from this interpolation procedure because no physical model is available in the *BaSeL* grid to accurately describe the atmosphere and the spectra of stars in these phases. For these reasons, in the files we assign an

arbitrary value (-99) to the magnitudes and the colours corresponding to these points. It has also to be pointed out that, because of some missing models in the *BaSeL* set of models near $T_{\text{eff}} \sim 11\,000$ K and $\log g \sim 1.5$, extrapolations in $\log g$ are necessary to compute the colours in this parameter range, leading to a few numerical approximations. As a consequence, the derived magnitudes and colours change more abruptly with T_{eff} than expected, and hence the shape of the stellar tracks do not appear very smooth in this region of the c-m diagram. For these peculiar points, we estimate our computed photometry to be accurate to about ± 0.05 mag.

³ The solar metallicity $[\text{Fe}/\text{H}] = 0$ is identified with the $Z = 0.02$ tracks. For other metallicities, we adopt the relation $[\text{Fe}/\text{H}] \equiv \log(Z/Z_{\odot})$, with $Z_{\odot} = 0.02$.

Table 3. Description of file extensions `ext` used for the stellar tracks (`mod*.ext`) and isochrones (`iso*.ext`)

File extension	description
<code>dat</code>	Complete set of predicted surface stellar properties
<code>UBVRIJHKLM</code>	Main stellar properties and photometric data for $(UBV)_J(RI)_C JHKLL'M$ system
<code>WFPC2</code>	Main stellar properties and photometric data for WFPC2 system
<code>geneva</code>	Main stellar properties and photometric data for Geneva system
<code>CMT1T2</code>	Main stellar properties and photometric data for Washington system

2.3.1. Absolute magnitudes and zero-points

The absolute magnitudes are computed from the absolute luminosity given in the tracks and the bolometric corrections computed from stellar atmosphere models. For *all* the photometric systems described in the following sections, we give the absolute magnitude, $M(V)$, expressed in the Johnson band. Absolute magnitudes in the other passbands can then be derived from the colour indices provided in the files. Our adopted bolometric correction scale is that described in Lejeune et al. (1998), defined in such a way to fit the empirical scale of Flower (1996) instead of using the unique calibration point of the Sun. Note that with this definition, we find $BC(V) = -0.108$ for the solar model of Kurucz (1992), a value slightly different of that usually quoted for the Sun.

The zero-points of the colours are defined from the Vega model spectrum of Kurucz (1992); for the $(UBV)_J(RI)_C JHKLL'M$, the CMT_1T_2 , and the HST-WFPC2 photometric systems, the computed colours for this model are set to zero, while for the Geneva system these values are adjusted on the observed photometry of Vega, $U - B = 1.505$, $B1 - B = 0.959$, $B2 - B = 0.900$, $V1 - B = 1.510$, $V^* - B = 1.662$, and $G - B = 2.168$ (Rufener 1976), and $V^* - V = 0.0^4$.

2.3.2. $(UBV)_J(RI)_C JHKLL'M$

For the Johnson-Cousins-Glass photometry, we used the filter response functions of Buser (1978) for (UBV) , Bessell (1979) for (RI) , and Bessell & Brett (1988) for $JHKLL'M$.

2.3.3. WFPC2

HST-WFPC2 synthetic photometry has been computed from the passbands described in the “*WFPC2 Instrument Handbook*”. We used the function responses⁵ from May 1998 which include the effects of all the detection chain (filter transmission, CCD quantum efficiency,

⁴ To avoid the confusion with the Johnson V band, the Geneva V^* is noted with an asterisk hereafter.

⁵ The tables can be retrieved from the STScI ftp site (ftp://ftp.stsci.edu/cdbs/cdbs8/synphot_tables/) as files `pcfxxxwsys.txt`, where `xxx` designates the mean filter wavelength in nm.

etc.), hence allowing direct comparisons of our synthetic c-m diagrams with HST data. The WFPC2 zero-points are usually defined on the *STMAG* system, based on a *constant-flux-density-per-unit-wavelength*. The conversion between the *VEGAMAG* system (based on the Vega’s spectrum) and the *STMAG* system is given by the following formula: $VEGAMAG = STMAG + 21.1 + 2.5 * \log(F_\nu(\text{Vega}))$ which, with our passband definitions and the Vega model spectrum of Kurucz, give the colour differences, $VEGAMAG - STMAG = -1.740, 1.514, 1.619,$ and 1.292 for F336W-F439W, F439W-F555W, F555W-F675W, and F675W-F814W respectively.

Colour-temperature and bolometric corrections using both the Lejeune et al. (1997) models and the Bessell et al. (1998) models have been presented by Origlia & Leitherer (2000). This paper also includes HST-NICMOS photometry and information on the transformation between WFPC2 and NICMOS and other systems.

2.3.4. Geneva photometry

The Geneva photometric indices, $U - B$, $B1 - B$, $B2 - B$, $V1 - B$, $V^* - B$, $G - B$, and $V^* - V$, have been computed using the latest revision of the Geneva passband definitions (Nicolet 1998, private communication). Differences with the passband functions previously published by Nicolet (1996) are very small, and do not exceed a few percents on the computed colours. In order to test the accuracy of our computed synthetic photometry, we made some comparisons with observed data for a sample of dwarf stars with $\log g \sim 3.5$ to 5 from the Rufener (1988) catalogue. The results have shown a good or very good agreement with the observations for most of the colour indices, with most of the colour differences $\lesssim 0.05$ mag. Larger deviations have been found in the UV (~ 0.1 to 0.2 mag near $T_{\text{eff}} = 8000$ K), and also for some peculiar multicolour parameters of the Geneva system, such as Δ and g .

2.3.5. Washington photometry

Washington broad-band photometry is often used in the studies of star clusters (see for instance Geisler & Sarajedini 1999; Lejeune & Buser 1999); and indeed provide very accurate photometric metallicity determinations for distant and extragalactic objects (Lejeune & Buser 2001, in preparation). We also give in the present

database, colour transformations in the Washington system (C, M, T_1, T_2), using the filter response functions published by Canterna & Harris (1979). The Cousins R band is very close to T_1 but has a higher efficiency, and hence could be a very good alternative to the Washington filter. For this reason, we provide in the files some Washington colours based on the R band instead T_1 , as suggested by Geisler (private communication).

2.3.6. Grids of colours

Complete grids of colours, computed from the whole *BaSeL-2.2* library for the photometric systems described above are available via anonymous ftp at the URL <ftp://tangerine.astro.mat.uc.pt/pub/BaSeL/>. In the near future, an interactive on-line service allowing such colour conversions for arbitrary sets of stellar parameters will be available at the URL <http://tangerine.astro.mat.uc.pt/BaSeL/>.

3. Database content and access

The database includes all stellar tracks listed in Col. 2 of Table 1 with a database ID. Corresponding isochrones covering the age range from 10^3 yr to 16 or 20 Gyr are also provided. In both cases the data contains the fundamental stellar parameters and all predicted surface properties. Files including the predicted synthetic photometry are provided for all tracks and isochrones. The organisation, nomenclature, and content of the respective files is discussed in the following.

3.1. Stellar tracks

The stellar tracks are grouped in files named according to the following conventions: `modIzzz.ext`, where **I** stands for the database ID (Col. 2, Table 1), **zzz** for the metallicity, and **ext** for the extension specifying the type of data (see Table 3). For example `modc001.WFPC2` contains the WFPC2 photometric data for all stellar tracks of the model grid # 2.

Grids 1–16 are included integrally in the database. The files with the ID “c” or “e” contain the $1.25 M_{\odot}$ track calculated *with* overshooting. The corresponding *no* overshoot model is found in the “o” files, as indicated in Col. 9 of Table 1. The “l” model set, providing the most appropriate low mass star models, consist of the following combination of tracks: $0.4\text{--}1 M_{\odot}$ main sequence tracks from Paper VIII (grids 15, 17 respectively), post-He flash models for 0.9 and $1 M_{\odot}$ from Paper VI (with ages properly adjusted to the calculations of Paper VIII), 1.25 (no overshoot), 1.5 , and $1.7 M_{\odot}$ tracks from Paper VI (grids 13, 14 respectively), and 2 and $2.5 M_{\odot}$ tracks from Paper I (grids 2, 5).

Obviously some of the sets in the database contain redundant data. This is due to the organisation of the sets designed for a simple and convenient use. See Sect. 4 for some recommendations on how to use the database.

The content of the various files is as follows:

- ***.dat** files: Predicted *surface* stellar properties using the table format described in Paper I (Cols. 1–15), complemented by the stellar core temperature for Wolf-Rayet stars or T_{eff} otherwise (Col. 16), and the mass loss rate ($\log \dot{M}$ in M_{\odot}/yr ; Col. 17). Columns 1–15 contain the following values: ID of evolutionary point (Col. 1), age (2), present mass (3), $\log L/L_{\odot}$ (4), $\log T_{\text{eff}}$ (5), and the surface abundances in mass fraction of H, ^4He , ^{12}C , ^{13}C , ^{14}N , ^{16}O , ^{17}O , ^{18}O , ^{20}Ne , and ^{22}Ne (Cols. 6–15). The *central* properties are given in the tables of the original papers.
- ***.UBVRIJHKLM** files: ID of evolutionary point (Col. 1), age (2), present mass (3), $\log T_{\text{eff}}$ (4), $\log g$ (5), $\log L/L_{\odot}$ (6), $M(V)$ (7), $U - B$ (8), $B - V$ (9), $V - R$ (10), $V - I$ (11), $V - K$ (12), $R - I$ (13), $I - K$ (14), $J - H$ (15), $H - K$ (16), $K - L$ (17), $J - K$ (18), $J - L$ (19), $J - L2$ (20), $K - M$ (21).
- ***.WFPC2** files: ID of evolutionary point (Col. 1), age (2), present mass (3), $\log T_{\text{eff}}$ (4), $\log g$ (5), $\log L/L_{\odot}$ (6), $M(V)$ (7), F336W-F439W (8), F439W-F555W (9), F555W-F675W (10), F555W-F814W (11), F675W-F814W (12), F439W-V (13).
- ***.geneva** files: ID of evolutionary point (Col. 1), age (2), present mass (3), $\log T_{\text{eff}}$ (4), $\log g$ (5), $\log L/L_{\odot}$ (6), $M(V)$ (7), $U - B$ (8), $B1 - B$ (9), $B2 - B$ (10), $V1 - B$ (11), $V^* - B$ (12), $G - B$ (13), $B1 - B2$ (14), $B2 - V1$ (15), $V1 - G$ (16), $V^* - V$ (17).
- ***.CMT1T2** files: ID of evolutionary point (Col. 1), age (2), present mass (3), $\log T_{\text{eff}}$ (4), $\log g$ (5), $\log L/L_{\odot}$ (6), $M(V)$ (7), $C - M$ (8), $M - T_1$ (9), $T_1 - T_2$ (10), $C - T_1$ (11), $M - T_2$ (12), $C - R$ (13), $M - R$ (14), $R - T_2$ (15), $V - T_1$ (16).

3.2. Isochrones

For each of the database sets a large number of isochrones have been calculated. A summary of the available data, together with the covered age range is shown in Table 2. Isochrones are provided for timesteps of $\Delta \log t = 0.05$ for ages above 1 Myr ($\log t = 6.0$). For younger ages isochrones are available for $\log t = 3.0, 5.0, 5.3, 5.6, 5.8,$ and 5.9 yr.

The isochrones are grouped in files named according to the following conventions: `iso_Izzz_ffff_tttt.ext`, where **I** stands for the database ID (Col. 2), **zzz** for the metallicity, **ffff** and **tttt** indicate the logarithmic age range (from – to) covered by isochrones, and **ext** for the extension specifying the type of data (see Table 3). For example `iso_c001_0300_1020.UBVRIJHKLM` includes the $(UBV)_J(RI)_C JHKLL'M$ photometry of all isochrones with ages from 10^3 yr to $10^{10.2}$ yr (~ 15.8 Gyr) of grid # 2.

The content of the files is the same as for the stellar tracks described above, with the following exceptions: Col. 1 is replaced by a line number, and Col. 2 now gives the initial mass along the isochrone.

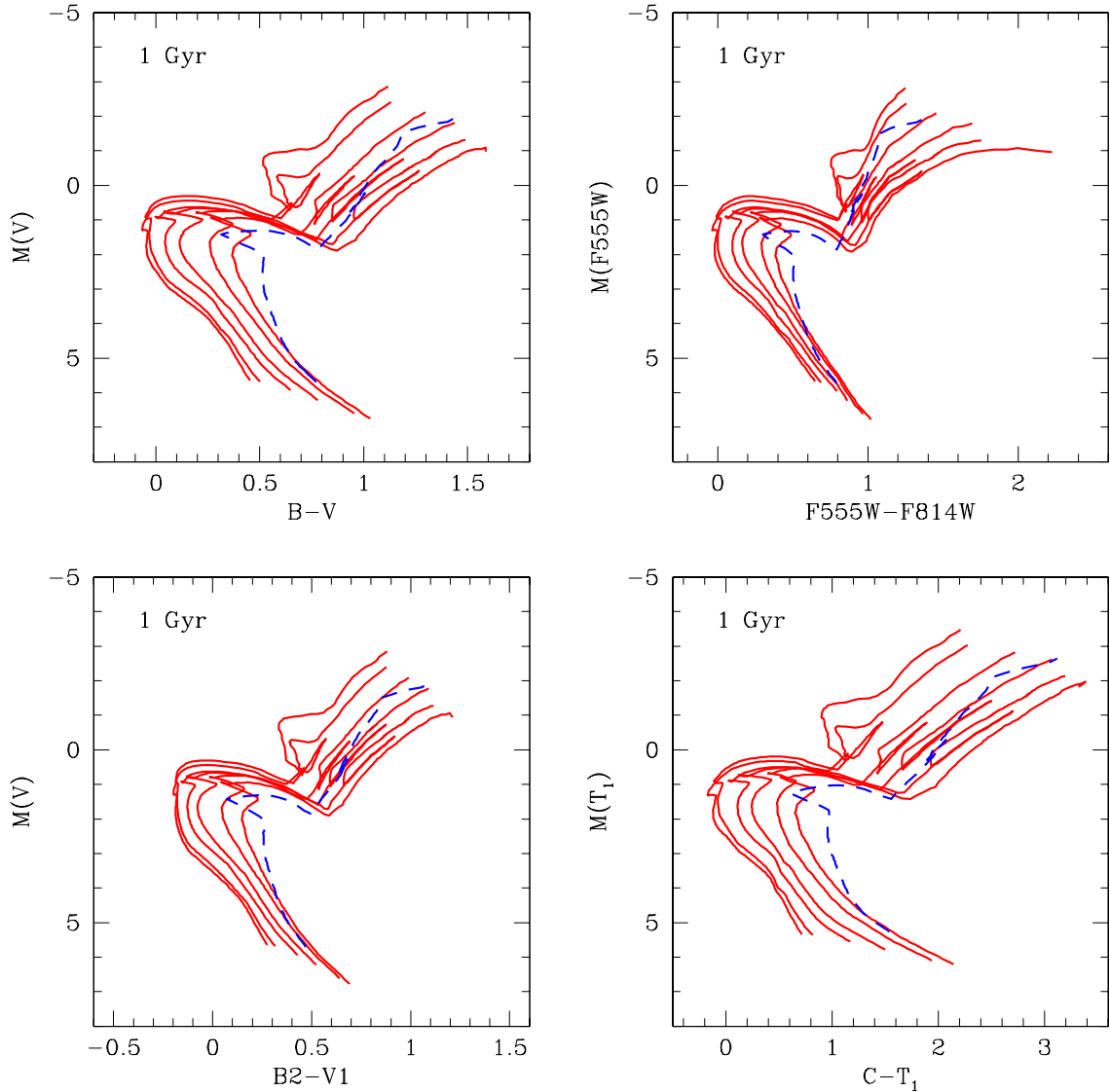


Fig. 1. Synthetic colour-magnitude diagrams in different observationnal planes (upper left: Johnson, upper right: HST-WFPC2, lower left: Geneva, lower right: Washington system) for the 1 Gyr isochrones at different metallicities: from left to right in each panel, $Z = 0.0004, 0.001, 0.004, 0.008, 0.02, 0.04$, and $Z = 0.1$ (dashed line)

3.3. Illustrations

In Fig. 1, we give an illustration of some synthetic c-m diagrams obtained from the present database. The figure shows in various planes the 1 Gyr isochrones at the different metallicities available ($Z = 0.0004, 0.001, 0.004, 0.008, 0.02, 0.04$, and 0.1). The peculiar behaviour of the $Z = 0.1$ isochrone is due to the overluminosity and the hotter temperature of these very metal-rich stars discussed in detail in Mowlavi et al. (1998a,b).

3.4. Access to database

The data will be accessible through the CDS⁶ and on the Web page <http://webast.ast.obs-mip.fr/stellar/>.

⁶ <http://cdsweb.u-strasbg.fr/cgi-bin/qcat?J/A+A/366/538>

Future updates of the database, including e.g. additional photometric systems, are foreseen through the latter site.

4. Recommendations for use

We now briefly indicate the most appropriate set of models for the cases where several choices are offered.

For most purposes the “basic model set” (files with the ID “c”) should be appropriate. The tracks of this set have e.g. been applied to analysis of Galactic open clusters with ages ~ 4 Myr–9.5 Gyr by Meynet et al. (1993).

For analysis of massive stars ($M_{\text{initial}} \gtrsim 12 M_{\odot}$) the high mass loss models (ID: “e”) should preferentially be used (see Maeder & Meynet 1994).

For studies of low mass stars ($M_{\text{initial}} \sim 0.4\text{--}2.5 M_{\odot}$) the combined model set (ID: “l”) at $Z = 0.001$ and $Z = 0.02$ should be most appropriate since it includes the MHD equation of state for $M \leq 1 M_{\odot}$ and covers also the

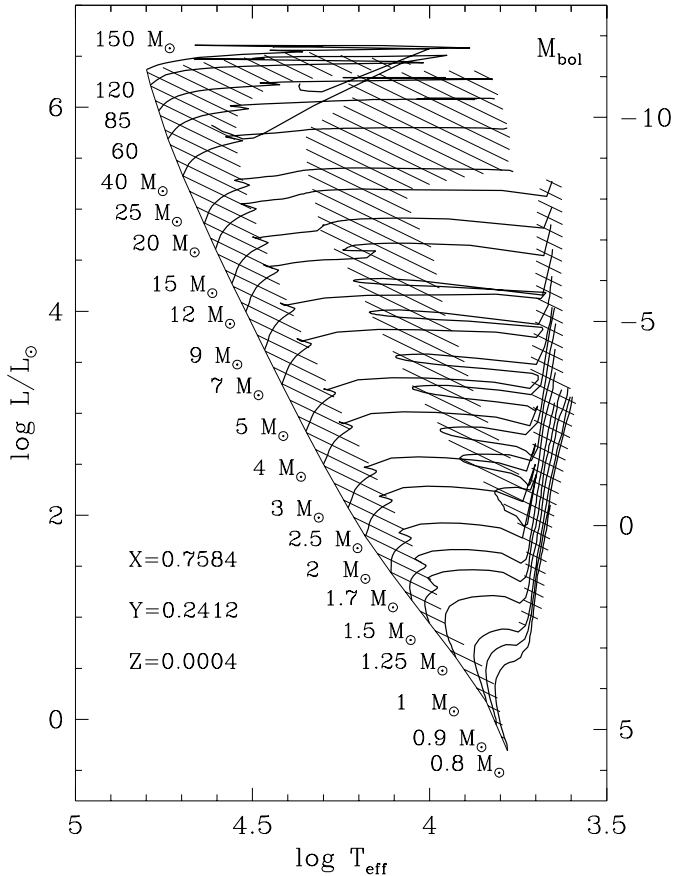


Fig. A1. Theoretical HR diagram for the ensemble of the calculated models for metallicity $Z = 0.0004$ with an overshooting parameter $d/H_p = 0.20$. The slow phases of nuclear burning are indicated by hatched areas. The $1.25 M_\odot$ track corresponds to the model without overshooting

post-helium flash evolutionary phases of stars with masses $0.8 \leq M/M_\odot \leq 1.7$.

For studies limited to the lowest masses ($M \leq 1 M_\odot$) the “m” set should be preferred.

For studies critical to the properties of stars in the mass range $1\text{--}1.5 M_\odot$, corresponding to the appearance of core convection on the main sequence, the “o” sets allow in comparison with the basic sets (“c”) to study the effect of enhanced convective cores (overshooting) in this mass range.

As mentioned earlier, the Geneva stellar grids used in this work do not include thermally pulsing AGB stars and post-AGB phases, such as central stars of planetary nebulae (CSPN) and white dwarfs (WD). If necessary the present data must be complemented with existing calculations from the literature. For recent calculations of AGB stars we refer e.g. to the complete or combined complete + synthetic models of Vassiliadis & Wood (1993); Blöcker (1995a); Forestini & Charbonnel (1997); and Langer et al. (1999), and to the synthetic models of Van den Hoeck & Groenewegen (1997) and Marigo et al. (1998). Recent models of CSPN and WD are given by e.g. Blöcker (1995b); Driebe et al. (1998), and Hansen & Phinney (1998).

Table A1. Lifetimes in nuclear phases (in units of 10^6 yr) for $Z = 0.0004$

Initial mass	H-burning phase	He-burning phase	C-burning phase	$\frac{t_{\text{He}}}{t_{\text{H}}}$
150 M_\odot	2.7239	0.2882	0.0056	0.1058
120	2.8937	0.3183	0.0053	0.1100
85	3.3192	0.3033 ¹	0.004 ¹	0.0882
60	3.9456	0.3359	0.0036	0.0851
40	5.0948	0.4169	0.0055	0.0818
25	7.5571	0.6235	0.0099	0.0825
20	9.5360	0.8028	0.015 ¹	0.0842
15	13.4686	1.1523	0.0240	0.0856
12	18.3778	1.5782	0.0436	0.0859
9	29.0134	2.5926	0.0909	0.0894
7	45.2717	4.4674	—	0.0987
5	86.8714	10.1487	—	0.1168
4	137.3413	18.8569	—	0.1373
3	259.7664	41.2311	—	0.1587
2.5	399.8616	75.6684	—	0.1892
2	706.4008	136.2883	—	0.1929
1.7	1110.0520	—	—	—
1.5	1603.4858	—	—	—
1.25 $\alpha = 0.2$	2827.6495	—	—	—
1.25 $\alpha = 0.0$	2623.3869	—	—	—
1	6008.6523	—	—	—
0.9	8963.7673	—	—	—
0.8	14095.3710	—	—	—

¹ estimated (cf. text)

Appendix A: Grid of stellar models at $Z = 0.0004$

A new grid of stellar models at very low metallicity (1/50 solar) has been calculated by one of us for various applications (see de Mello et al. 1998; Stasińska & Schaerer 1999). The full grid of stellar tracks from 0.8 to $150 M_\odot$ is briefly summarised here.

The input physics is identical to that of Meynet et al. (1994, Paper V). This includes in particular the adoption of “high” mass loss rates, i.e. $\dot{M} = 8 \cdot 10^{-5} M_\odot/\text{yr}$ for WNL stars and twice the mass loss rates of de Jager et al. (1988) for stars with $M_{\text{initial}} \geq 3 M_\odot$. Otherwise we follow the prescription of Paper I. For consistence with the earlier grids the initial composition is calculated as in Paper I: $X = 0.7584$, $Y = 0.2412$, $Z = 0.0004$.

The HRD with the calculated tracks is shown in Fig. A1. Hatched areas indicate regions of slow nuclear burning phases. The H, He, and C burning lifetimes are given in Table A1. Due to numerical instabilities the $85 M_\odot$ model could not be fully evolved to the end of He burning. The remaining He-burning lifetime as well as the duration of C-burning were estimated by interpolation between the two adjacent tracks. For similar reasons t_{C} of the $20 M_\odot$ model had also to be estimated.

The mass limit for the formation of WR stars, M_{WR} , at $Z = 0.0004$ from the present tracks is $M_{\text{WR}} \sim 85 M_\odot$, as already derived in de Mello et al. (1998). Other properties of the $Z = 0.0004$ models can readily be derived from the detailed data included in the present database.

Acknowledgements. We thank G. Burki, N. Cramer and B. Nicolet for help with the Geneva photometric system. We have benefited from useful discussions with R. Buser, C. Charbonnel, A. Maeder, J.-C. Mermilliod, and G. Meynet. E. Grebel and E. Tolstoy provided some early user feedback on the database. TL gratefully acknowledges financial support from the Swiss National Science Foundation (grant 20-53660.98 to Prof. Buser) and from the “Fundação para a Ciência e Tecnologia” (Portugal), (grant PRAXIS-XXI/BPD/22061/99).

References

- Alexander, D. R., & Ferguson, J. W. 1994, *ApJ*, 437, 879
 Baraffe, I., Chabrier, G., Allard, F., & Hauschildt, P. H. 1995, *ApJ*, 446, L35
 Bernasconi, P. A. 1996, *A&AS*, 120, 57
 Bertelli, G., Bressan, A., Chiosi, C., Fagotto, F., & Nasi, E. 1994, *A&AS*, 106, 275
 Bessell, M. S. 1979, *PASP*, 91, 589
 Bessell, M. S., & Brett, J. M. 1988, *PASP*, 100, 1134
 Bessell, M. S., Castelli, F., & Plez, B. 1998, *A&A*, 333, 231
 Blöcker, T. 1995a, *A&A*, 297, 727
 Blöcker, T. 1995b, *A&A*, 299, 755
 Buser, R. 1978, *A&A*, 62, 425
 Canterna, R., & Harris, D. 1979, *AJ*, 84, 1750
 Castor, J. I., Abbott, D. C., & Klein, R. I. 1975, *ApJ*, 195, 157
 Charbonnel, C., Däppen, W., & Schaerer, D. 1999, *A&AS*, 135, 405, Paper VIII
 Charbonnel, C., Meynet, G., Maeder, A., Schaller, G., & Schaerer, D. 1993, *A&AS*, 101, 415, Paper III
 Charbonnel, C., Meynet, G., Maeder, A., & Schaerer, D. 1996, *A&AS*, 115, 339, Paper VI
 de Jager, C., Nieuwenhuijzen, H., & van der Hucht, K. A. 1988, *A&AS*, 72, 259
 de Mello, D., Schaerer, D., Heldmann, J., & Leitherer, C. 1998, *ApJ*, 507, 199
 Driebe, T., Schoenberner, D., Blöcker, T., & Herwig, F. 1998, *A&A*, 339, 123
 Flower, P. J. 1996, *ApJ*, 469, 355
 Forestini, M., & Charbonnel, C. 1997, *A&AS*, 123, 241
 Geisler, D. 1984, *PASP*, 96, 723
 Geisler, D., & Sarajedini, A. 1999, *AJ*, 117, 308
 Girardi, L., Bressan, A., Chiosi, C., Bertelli, G., & Nasi, E. 1996, *A&AS*, 117, 113
 Hansen, B. M. S., & Phinney, E. S. 1998, *MNRAS*, 294, 569
 Kurucz, R. L. 1991, in *Stellar Atmospheres: Beyond Classical Models*, NATO ASI Series C, vol. 341, ed. L. Crivellari, I. Hubeny, & D. G. Hummer, 441
 Kurucz, R. L. 1992, in *Stellar Populations of Galaxies*, ed. B. Barbuy, & A. Renzini (Dordrecht, Kluwer), 22
 Langer, N. 1989, *A&A*, 220, 135
 Langer, N., Heger, A., Wellstein, S., & Herwig, F. 1999, *A&A*, 346, L37
 Leitherer, C., et al. 1996, *PASP*, 108, 996
 Lejeune, T., & Buser, R. 1999, in *Spectrophotometric dating of stars and galaxies*, ed. I. Hubeny, S. Heap, & R. Cornett, ASP Conf. Ser., 192, 211
 Lejeune, T., Cuisinier, F., & Buser, R. 1997, *A&AS*, 125, 246
 Lejeune, T., Cuisinier, F., & Buser, R. 1998, *A&AS*, 130, 75
 Marigo, P., Bressan, A., & Chiosi, C. 1998, *A&A*, 331, 564
 Maeder, A., & Meynet, G. 1989, *A&A*, 210, 155
 Maeder, A., & Meynet, G. 1994, *A&A*, 287, 803
 Meynet, G., Maeder, A., Schaller, G., Schaerer, D., & Charbonnel, C. 1994, *A&AS*, 103, 97, Paper V
 Meynet, G., Mermilliod, J.-C., & Maeder, A. 1993, *A&AS*, 98, 477
 Mihalas, D., Hummer, D. G., & Däppen, W. 1988, *ApJ*, 331, 815
 Mowlavi, N., Schaerer, D., Meynet, G., Bernasconi, P. A., Charbonnel, C., & Maeder, A. 1998a, *A&AS*, 128, 471, Paper VII
 Mowlavi, N., Meynet, G., Maeder, A., Schaerer, D., & Charbonnel, C. 1998b, *A&A*, 335, 573
 Nicolet, B. 1996, *Baltic Astron.*, 5, 417
 Origlia, L., & Leitherer, C. 2000, *AJ*, 119, 2018
 Reimers, D. 1975, *Mem. Soc. Roy. Sci. Liège*, 8, 369
 Rufener, F. 1988, *Catalogue of Stars measured in the Geneva Observatory Photometric System*, fourth edition, Observatoire de Genève, Sauverny, Switzerland
 Rufener, F. 1976, *A&AS*, 26, 275
 Salasnich, B., Girardi, L., Weiss, A., & Chiosi, C. 2000, *A&A*, 361, 1023
 Schaerer, D., Charbonnel, C., Meynet, G., Maeder, A., & Schaller, G. 1993, *A&AS*, 102, 339, Paper IV
 Schaerer, D., de Koter, A., Schmutz, W., & Maeder, A. 1996, *A&A*, 312, 475
 Schaerer, D., Meynet, G., Maeder, A., & Schaller, G. 1993, *A&AS*, 98, 523, Paper II
 Schaller, G., Schaerer, D., Meynet, G., & Maeder, A. 1992, *A&AS*, 96, 269, Paper I
 Stasińska, G., & Schaerer, D. 1999, *A&A*, 351, 72
 Van den Berg, D. A. 1985, *ApJS*, 58, 711
 Van den Hoek, L. B., & Groenewegen, M. A. T. 1997, *A&AS*, 123, 305
 Vassiliadis, E., & Wood, P. R. 1993, *ApJ*, 413, 641
 Westera, P., Lejeune, T., & Buser, R. 1999, in *Spectrophotometric dating of stars and galaxies*, ed. I. Hubeny, S. Heap, & R. Cornett, ASP Conf. Ser., 192, 203, Annapolis, Maryland, USA